Ceiling Jet Flows

14

Ronald L. Alpert

Introduction

Much of the hardware associated with detection and suppression of fire in commercial, manufacturing, storage, and modern residential buildings is located near the ceiling surfaces. In case of a fire, hot gases in the fire plume rise directly above the burning fuel and impinge on the ceiling. The ceiling surface causes the flow to turn and move horizontally under the ceiling to other areas of the building remote from the fire position. The response of smoke detectors, heat detectors, and sprinklers installed below the ceiling so as to be submerged in this hot flow of combustion products from a fire provides the basis for building fire protection.

Studies quantifying the flow of hot gases under a ceiling resulting from the impingement of a fire plume have been conducted since the 1950s. Studies at the Fire Research Station in Great Britain [1, 2], Factory Mutual Research Corporation [3–7], the National Institute of Standards and Technology (NIST) [8, 9], and at other research laboratories [10, 11] have sought to quantify the gas temperatures and velocities in the hottest portion of the flow produced by steady fires beneath smooth, unconfined horizontal ceilings.

Ceiling jet refers to the relatively rapid gas flow in a shallow layer beneath the ceiling surface that is driven by the buoyancy of the hot combustion products from the plume. Figure 14.1 shows an idealization of an axisymmetric ceiling jet flow at varying radial positions, r, beneath an unconfined ceiling. In actual fires within buildings, the simple conditions pictured—a hot, rapidly moving gas layer sandwiched between the ceiling surface and tranquil, ambient-temperature air—exist only at the beginning of a fire, when the quantity of combustion gases produced is not sufficient to accumulate into a stagnant, heated gas layer in the upper portion of the compartment. Venting the ceiling jet flow through openings in the ceiling surface or edges can retard the accumulation of this heated gas layer.

As shown in Fig. 14.1, the ceiling jet flow emerges from the region of plume impingement on the ceiling, flowing radially away from the fire. As it does, the layer grows thicker by entraining room air at the lower boundary. This entrained air cools the gases in the jet and reduces its velocity. As the hot gases move out across the ceiling, heat transfer cools the portion adjacent to the ceiling surface.

Steady Flow Under Horizontal, Unconfined Ceilings

Weak Plume-Driven Flow Field

A generalized theory to predict gas velocities, gas temperatures, and the thickness (or depth) of a steady fire-driven ceiling jet flow has been developed by Alpert [4] for the case of a weak

R.L. Alpert (✉)
Alpert FireProtection Science

M. Hurley (ed.), *SFPE Handbook of Fire Protection Engineering*,
DOI 10.1007/978-1-4939-2565-0_14,

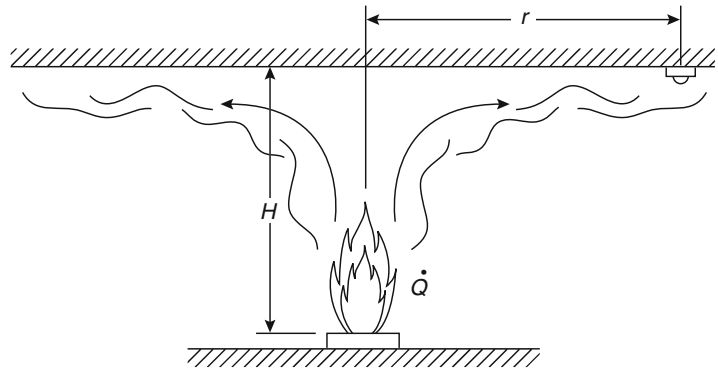

Fig. 14.1 Ceiling jet flow beneath an unconfined ceiling

plume, when flame height is much less than the height, H, of the ceiling above the burning fuel. This work involves the use of several idealizations in the construction of the theoretical model, but results are likely to provide reasonable estimates over radial distances of one or two ceiling heights from the point of fire plume impingement on the ceiling.

Ceiling Jet Thickness Alpert defined the thickness of the ceiling jet, ℓ_T, as the distance below the ceiling where the excess of gas temperature above the ambient value, ΔT, drops to $1/e$ (1/2.718 ...) of the maximum excess temperature. Based on this definition, measurements obtained with a liquid pool fire 8 m beneath a ceiling show that ℓ_T/H is about 0.075 at an r/H of 0.6, increasing to a value of 0.11 for r/H from about 1 to 2. These results are in good agreement with detailed measurements and analysis for the region $r/H < 2$ performed by Motevalli and Marks [12] during their small-scale (0.5- and 1.0-m ceiling heights) experiments. The following correlation for ℓ_T/H developed by Motevalli and Marks from their temperature data confirms the predicted constancy of ceiling jet thickness (at about 10–12 % of H) for r/H from Alpert's theory:

$$\frac{\ell_T}{H} = 0.112\left[1 - \exp\left(-2.24\frac{r}{H}\right)\right] \quad \text{for } 0.26 \le \frac{r}{H} \le 2.0 \tag{14.1}$$

Additional measurements of ceiling jet thickness, for steady flows induced by strong plumes and for transient flows, are discussed later.

Within the ceiling jet flow, the location of maximum excess temperature and velocity are predicted [4] to be highly scale dependent, even after normalization by the ceiling height. Measurements of the distance below the ceiling at which these maxima occur have been made mainly for 1-m scale experiments [12, 13]. Results show distances below the ceiling ranging from about 1 % to 2 % of the ceiling height for r/H from less than 1 to 2, with predicted reductions in the percent of ceiling height at larger scales.

Much of the discussion below deals with predictions and correlations of the maximum excess temperature and velocity in the ceiling jet flow, which occur, as already noted, relatively close to the ceiling surface. Often fire detectors or sprinklers are placed at ceiling standoff distances that are outside of this region and therefore will experience cooler temperatures and lower velocities than predicted. In facilities with very high ceilings, the detectors could be closer to the ceiling than 1 % of the fire source-to-ceiling separation and will fall in the ceiling jet thermal and viscous boundary layers. In low-ceiling facilities, it is possible for sprinklers or detectors to be placed outside of the ceiling jet flow entirely if the standoff is greater than 12 % of the fire source-to-ceiling height. In this case, response time could be drastically increased.

Ceiling Jet Excess Temperature and Velocity Alpert [3] has developed easy-to-use correlations to quantify the maximum excess gas temperature (above the ambient value) and velocity at a given position in a ceiling jet flow

produced by a steady fire. These correlations are widely used in hazard analysis calculations. Evans and Stroup [14] have employed the correlations in the development of a generalized program to predict heat detector response for the case of a detector totally submerged in the ceiling jet flow. The correlations are based on measurements collected during fire tests involving fuel arrays of wood and plastic pallets, empty cardboard boxes, plastic materials in cardboard boxes, and liquid fuels. Heat release rates for these fuels range from 600 kW to 98 MW, total ceiling heights range from 4.6 to 18 m, and radial positions for most measurements range out to a little more than twice the ceiling height. In SI units, Alpert's [3] correlations for maximum ceiling jet excess temperatures and velocities are as follows:

$$T - T_\infty = 16.9 \frac{\dot{Q}^{2/3}}{H^{5/3}} \qquad \text{for } r/H \leq 0.18 \tag{14.2}$$

$$T - T_\infty = 5.38 \frac{\dot{Q}^{2/3}/H^{5/3}}{(r/H)^{2/3}} \quad \text{for } r/H > 0.18 \tag{14.3}$$

$$U = 0.947 \left(\frac{\dot{Q}}{H}\right)^{1/3} \qquad \text{for } r/H \leq 0.15 \tag{14.4}$$

$$U = 0.197 \frac{(\dot{Q}/H)^{1/3}}{(r/H)^{5/6}} \qquad \text{for } r/H > 0.15 \tag{14.5}$$

where temperature, T, is in °C; velocity, U, is in m/s; total heat release rate, $\dot{Q}$ is in kW; and radial position and ceiling height (r and H) are in m.

Data from these fire tests are correlated using the rate at which heat is actually released in the fire, $\dot{Q}$, based on measured fuel mass loss rates and the best estimates for actual heat of combustion that were available in 1970–1971. Even though it is the convective component of this total heat release rate that is directly related to the buoyancy of the fire, accurate estimates for this convective component were not readily available for all the fuels tested when the correlations were first developed. For the liquid alcohol pool fires that constitute the primary basis of the correlation developed by Alpert, the convective heat release rate, $\dot{Q}_c$, is now known to be about 74 % of the actual heat release rate. However, for the remaining solid commodities and pallets, the convective heat release rate varies from about 60 % to 70 % of the actual heat release rate for mixed plastic/cardboard commodities and wood, respectively, with flammable liquids similar to heptane being in the middle of this range. Hence, for general commodities, it would be desirable to use ceiling jet excess temperature and velocity correlations based on convective heat release rate (see such correlations in Equations 14.7 and 14.8).

The preceding correlations for both temperatures and velocities (Equations 14.2, 14.3, 14.4, and 14.5) are broken into two parts. One part applies for the ceiling jet in the area of the impingement point where the upward flow of gas in the buoyant plume turns to flow out beneath the ceiling horizontally, with an assumed unchanged velocity magnitude. The impingement point or turning region correlations (Equations 14.2, 14.3 and 14.4) are independent of radius and represent plume temperatures

and velocities calculated at the ceiling height above the fire source. The other correlations (Equations 14.3 and 14.5) apply outside of this turning region as the flow moves away from the impingement area. It is important to recognize that these correlations implicitly assume that there is a point buoyancy source for the impinging plume located at the top surface of the burning fuel. Hence, there is no dependence on the horizontal dimension (e.g., effective diameter) of the fire source in the correlations, and the height of the fuel array is restricted to being a small fraction of the ceiling height.

In order to remedy deficiencies discussed above in the existing correlations, much of the original data from the 1970s has been reanalyzed by the author. This new analysis ignores a small number of measurements where an accurate estimate of convective heat release rate for the corresponding fire sources (plastic pallets and one cardboard box commodity) would be very difficult to obtain. For the remaining large-scale fire tests, the convective heat release rate is calculated from measurements of fuel mass loss rate and handbook values of the convective heat of combustion. Instead of arbitrarily correlating measurements with the ceiling elevation above the top fuel surface, H, the new analysis uses the ceiling elevation above the location of the virtual plume origin, $z_H - z_v$. The location, z_v, of the virtual plume origin above a reference location is given (see Chap. 13) by a correlation based on the actual heat release rate, $\dot{Q}$, and the effective diameter, D_{eff}, of the fuel array. When height in the plume, z, is measured from the base of the flame zone instead of the top surface of the burning fuel, the following expression for virtual origin height has been found to be applicable even to complex fuel arrays:

$$z_v = 0.083\dot{Q}^{2/5} - 1.02D_{\text{eff}} \tag{14.6}$$

In Equation 14.6, z_v is the distance above the base of a burning fuel array and D_{eff} is the diameter of a circle having the same plan area as for the actual array. The result of correlating excess temperature and velocity measurements from full-scale tests using the same functional relationships as in Equations 14.3 and 14.5 but based on $\dot{Q}_c$ instead of $\dot{Q}$ and $z_H - z_v$ instead of H is shown in Figs. 14.2 and 14.3. Further details of this reanalysis of ceiling jet data from the early 1970s is provided in a recent lecture by the author [15].

In Figs. 14.2 and 14.3, the ordinates are the dimensional quantities

$$\frac{(T - T_\infty)(z_H - z_v)^{5/3}}{\dot{Q}_c^{2/3}} \quad \text{and} \quad \frac{U(z_H - z_v)^{1/3}}{\dot{Q}_c^{1/3}}$$

respectively. Values for these ordinates at the plume axis (see Chap. 13) are shown for comparison with the ceiling jet values. Regression fits based on data only from the ethanol pool fires, for which heat release rates are known most accurately, are also shown in these figures. Based on the data from all of the full-scale fire tests, the following new correlations are obtained for excess gas temperature and velocity in the ceiling jet:

$$T - T_\infty = 7.22\frac{\dot{Q}_c^{2/3}}{(z_H - z_v)^{5/3}}\left(\frac{r}{z_H - z_v}\right)^{-0.678} \tag{14.7}$$

$$\text{for } \frac{r}{z_H - z_v} > 0.16$$

$$U = 0.229\frac{\dot{Q}_c^{1/3}}{(z_H - z_v)^{1/3}}\left(\frac{r}{z_H - z_v}\right)^{-1.017}$$

$$\text{for } \frac{r}{z_H - z_v} > 0.228 \tag{14.8}$$

where the limits on $\frac{r}{z_H - z_v}$ in Equations 14.7 and 14.8 are obtained from the respective intersections of the ceiling jet regression fits with the axis values shown from the plume correlations. Within the turning region (i.e., for $\frac{r}{z_H - z_v} \leq$ the limits shown) existing correlations for maximum temperature and velocity in the plume can be used.

A further improvement to the ceiling jet excess temperature and velocity correlations can be obtained [15] by using just the ethanol pool and heptane spray fire data, not only because these are the best documented fire

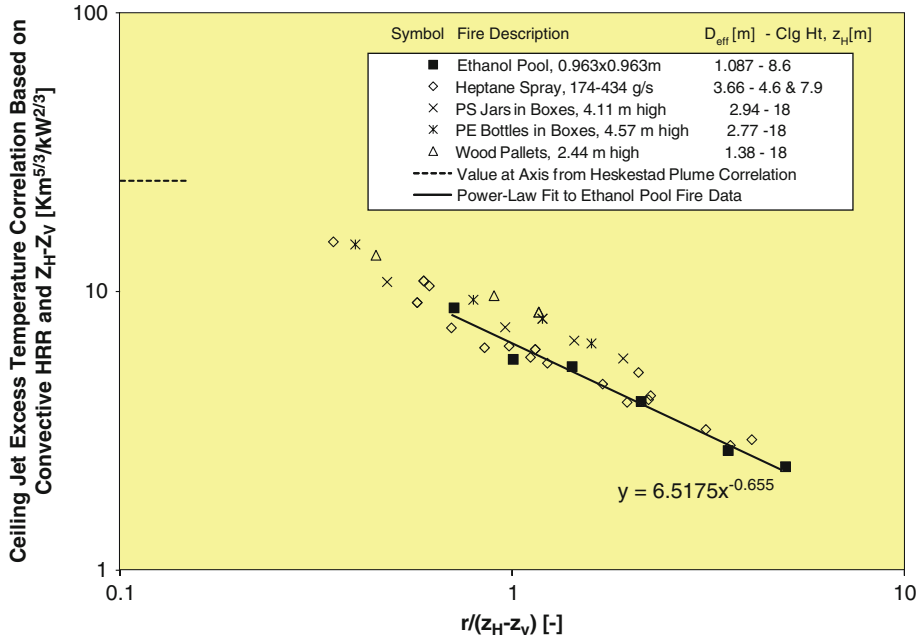

Fig. 14.2 Correlation of maximum ceiling jet excess temperature data from full-scale fire tests (Note that "PE bottles" previously was called "PVC bottles," an error discovered by comparing known test numbers involving the commodity with descriptions in a test report; Also note that previously, data for heptane sprays had not contained the virtual origin correction applied to data for the other commodities, due to a spreadsheet error)

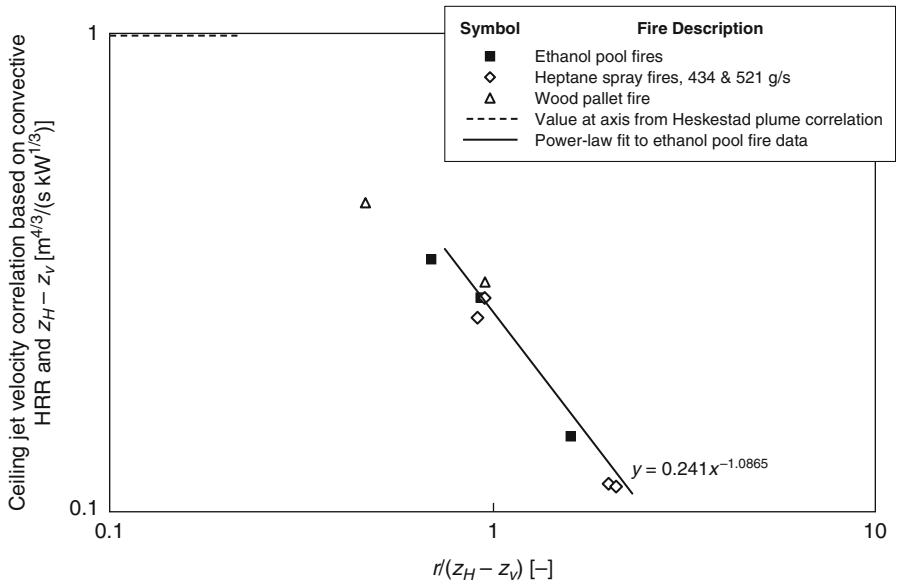

Fig. 14.3 Correlation of maximum ceiling velocity data from full-scale fire tests (See legend from Fig. 14.2)

sources from the original study, in terms of combustion parameters, but also because these are the only near steady-state fire sources. Fires in piles of solid fuels are inherently transient, which makes a data correlation difficult when transient velocity and temperature data are not available.

Modern handbook values [16] for actual and convective heats of combustion for the two fuels selected will now be used instead of what had been assumed (from the knowledge available at time) in the original ceiling-jet study. As a result, the value of $\dot{Q}$ is 13 % greater for ethanol and 8 % less for heptane compared to the values used for the correlations in Equations 14.7 and 14.8. With these new values, virtual source heights and convective heat release rates can be obtained [15]. For both the heptane spray and ethanol pool data taken together, the resulting regression fit equations and regression coefficients (R^2 values) are given below:

$$T - T_\infty = 6.721 \frac{\dot{Q}_c^{2/3}}{(z_H - z_v)^{5/3}} \left(\frac{r}{z_H - z_v} \right)^{-0.6545} \quad R^2 = 0.958 \quad \text{for} \frac{r}{z_H - z_v} > 0.134 \tag{14.7A}$$

$$U = 0.2526 \frac{\dot{Q}_c^{1/3}}{(z_H - z_v)^{1/3}} \left(\frac{r}{z_H - z_v} \right)^{-1.0739} \quad R^2 = 0.972 \quad \text{for} \frac{r}{z_H - z_v} > 0.246 \tag{14.8A}$$

Certain constraints should be understood when applying these correlations in the analysis of fire flows. The correlations apply only during times after fire ignition when the ceiling flow may be considered unconfined; that is, no accumulated warm upper layer is present. Walls close to the fire affect the temperatures and velocity in the ceiling jet independent of any effect on the fire-burning rate due to radiant heat received from the walls. The correlations were developed from test data to apply in cases where the fire source is at least a distance 1.8 times the ceiling height from the enclosure walls. For special cases where burning fuel is located against a flat wall surface or two wall surfaces forming a 90° corner, the correlations are adjusted based on the method of reflection. This method makes use of symmetry to account for the effects of the walls in blocking entrainment of air into the fire plume. For the case of a fire adjacent to a flat wall, $2\dot{Q}$ is substituted for $\dot{Q}$ in the correlations. For a fire in a 90° corner, $4\dot{Q}$ is substituted for $\dot{Q}$ in the correlations [3]. More accurate formulas for ceiling jet gas temperature, as well as ceiling heat flux, in a 90° corner that were obtained from experiments with a propane burner can be found in the section following on "Corner Configuration with Strong Plumes".

Experiments have shown that unless great care is taken to ensure that the fuel perimeter is in contact with the wall surfaces, the method of reflection used to estimate the effects of the walls on ceiling jet temperature will be inaccurate. For example, Zukoski et al. [17] found that a circular burner placed against a wall so that only one point on the perimeter contacted the wall behaved almost identically to a fire far from the wall with plume entrainment only decreasing by 3 %. When using Equations 14.2, 14.3, 14.4, and 14.5, this fire would be represented by replacing $\dot{Q}$ with $1.05\dot{Q}$ and not $2\dot{Q}$ as would be predicted by the method of reflections. The value of $2\dot{Q}$ would be appropriate for a semicircular burner with the entire flat side pushed against the wall surface.

Consider the following calculations, which demonstrate typical uses of the correlations, Equations 14.2, 14.3, 14.4, and 14.5.

(a) The maximum excess temperature under a ceiling 10 m directly above a 1.0-MW heat-release-rate fire is calculated using Equation 14.2 as

$$T - T_\infty = \frac{16.9(1000)^{2/3}}{10^{5/3}}$$
$$= \frac{16.9(100)}{46.42}$$
$$\Delta T = 36.4°\text{C}$$

(b) For a fire that is against noncombustible walls in a corner of a building and 12 m below the ceiling, the minimum heat release rate needed to raise the temperature of the gas below the ceiling 50 °C at a distance 5 m from the corner is calculated using Equation 14.3 and the symmetry substitution of $4\dot{Q}$ for $\dot{Q}$ to account for the effects of the corner as

$$T - T_\infty = 5.38\frac{(4\dot{Q})^{2/3}/H^{5/3}}{(r/H)^{2/3}}$$
$$50 = 5.38\frac{(4\dot{Q})^{2/3}}{12^{5/3}(5/12)^{2/3}}$$
$$\dot{Q} = \frac{5}{4}\left[\frac{50(12)}{5.38}\right]^{3/2}$$
$$\dot{Q} = 1472\ \text{kW} = 1.472\,\text{MW}$$

(c) The maximum velocity at this position is calculated from Equation 14.5, modified to account for the effects of the corner as

$$U = 0.197\frac{(4\dot{Q}/H)^{1/3}}{(r/H)^{5/6}}$$
$$= \frac{0.197(5888)^{1/3}}{(5/12)^{5/6}12^{1/3}}$$
$$U = 3.2\ \text{m/s}$$

Nondimensional Ceiling Jet Relations Heskestad [7] developed correlations[1] for maximum ceiling jet excess temperature and velocity based on alcohol pool-fire tests performed at the U.K. Fire Research Station in the 1950s. These correlations are cast in the following heat release rate, excess temperature, and velocity variables that are nondimensional (indicated by the superscript asterisk) and applicable to steady-state fires under unconfined ceilings (indicated by the subscript 0):

$$\dot{Q}_0^* = \frac{\dot{Q}}{\rho_\infty c_p T_\infty g^{1/2} H^{5/2}} \tag{14.9}$$

$$\Delta T_0^* = \frac{\Delta T/T}{\left(\dot{Q}_0^*\right)^{2/3}} \tag{14.10}$$

$$U_0^* = \frac{U/\sqrt{gH}}{\left(\dot{Q}_0^*\right)^{1/3}} \tag{14.11}$$

Figure 14.4 shows a plot of the Heskestad correlation for excess temperature and velocity data as solid line curves. The correlations developed by Alpert [3] are plotted as broken curves, using the same dimensionless parameters with assumed ambient temperature of 293 K (20 °C), normal atmospheric pressure, and convective heat release rate equal to the total heat release rate, $\dot{Q}_c = \dot{Q}$. Generally, the results of Heskestad [7] predict slightly higher excess temperatures and substantially greater gas velocities than Alpert's [3] results. Another curve shown in Fig. 14.2 is a fit to the mean ceiling jet velocity predicted by the generalized theory of Alpert [4], which also predicts that the turning-region boundary should be at $r/H = 0.17$. This predicted velocity is reasonably close to Heskestad's [7] experimental correlation for velocity. Based on the results shown in Fig. 14.4, the nondimensional excess temperature from the Heskestad [7] correlation and the nondimensional velocity from Alpert's theory [4, 13] are recommended for the prediction of steady ceiling jet flows beneath unobstructed ceilings. The Heskestad correlation and the Alpert theory are adequately fit, respectively, by the following expressions:

[1] Originally developed by G. Heskestad and C. Yao in "A New Approach to Development of Installation Standards for Fired Detectors," *Technical Proposal No. 19574,* prepared for The Fire Detection Institute, by Factory Mutual Research Corporation, Norwood, MA (1971).

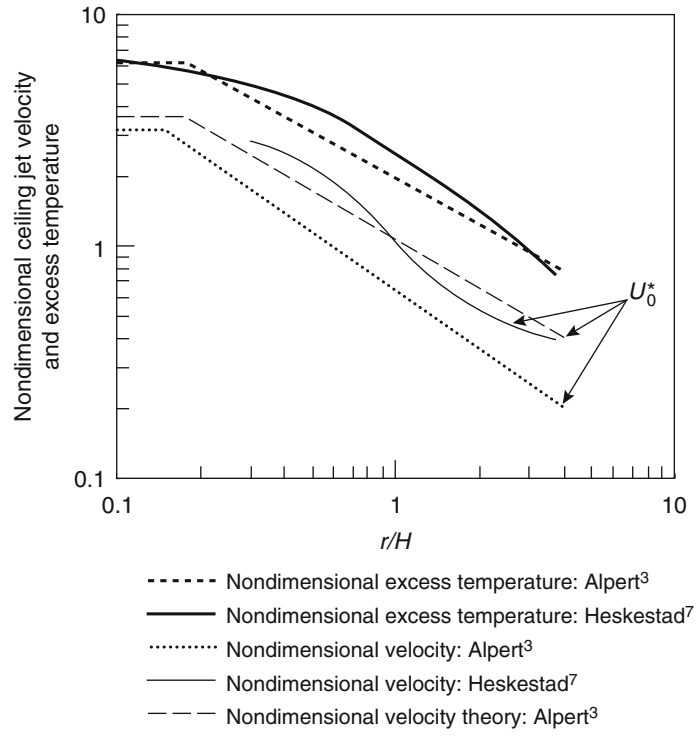

Fig. 14.4 Dimensionless correlations for maximum ceiling jet temperatures and velocities produced by steady fires. *Solid line*: Heskestad [7]; *dotted line*: Alpert [3]

$$\Delta T_0^* = \left(0.225 + 0.27\tfrac{r}{H}\right)^{-4/3} \quad \text{for } 0.2 \le r/H < 4.0 \tag{14.12}$$

$$\Delta T_0^* = 6.3 \quad \text{for } r/H \le 0.2 \tag{14.13}$$

$$U_0^* = 1.06\left(\frac{r}{H}\right)^{-0.69} \quad \text{for } 0.17 \le r/H < 4.0 \tag{14.14}$$

$$U_0^* = 3.61 \quad \text{for } r/H \le 0.17 \tag{14.15}$$

Heskestad and Delichatsios [18] examined the original data from Heskestad [7] and concluded that nondimensional velocity and temperature could be related by the following equation:

$$\frac{U_0^*}{\sqrt{\Delta T_0^*}} = 0.68\left(\frac{r}{H}\right)^{-0.63} \quad \text{for } r/H \ge 0.3 \tag{14.16}$$

The preceding relation has been found applicable to a much wider range of conditions than just steady-state alcohol pool fires having weakly buoyant plumes. For example, this relationship between ceiling jet velocity and excess temperature is consistent with measurements [18] for time-dependent fires having strong plumes.

Other methods used to calculate ceiling jet velocity and maximum possible (when the ceiling is adiabatic) ceiling jet temperatures are reported by Cooper and Woodhouse [9]. A critical review of correlation formulas for excess temperature and velocity in the ceiling jet under

a variety of conditions has been assembled by Beyler [19]. To apply these and the preceding expressions to realistic burning situations, it is recommended that the convective heat release rate should be used.

Strong Plume-Driven Flow Field

When the flame height of a fire plume is comparable to the height of the ceiling above the burning fuel, the resultant ceiling jet is driven by a strong plume. Additional information about this type of flow field is provided in the section on "Sloped Ceilings" (see the special case of zero inclination angle, i.e., a horizontal ceiling).

Ceiling Jet Temperature Heskestad and Hamada [6] measured ceiling jet temperatures for ratios of free flame height (in the absence of a ceiling, obtained from existing knowledge of flame heights) to ceiling height ranging from 0.3 up to 3. A correlation of excess temperatures could be achieved by using the plume radius, b, at the ceiling as a normalizing length scale, rather than the ceiling height used for the case of a weak plume. This correlation takes the form:

$$\frac{\Delta T}{\Delta T_p} = 1.92\left(\frac{r}{b}\right)^{-1} - \exp\left[1.61\left(1-\frac{r}{b}\right)\right] \quad \text{for } 1 \le \frac{r}{b} \le 40 \tag{14.17}$$

where ΔT_p is the excess temperature on the plume centerline at the level of the ceiling (obtained from Equations 14.2 or 14.13 or other fire-plume relations) and b is the radius where the velocity of the impinging plume is one-half the centerline value. The expression for this characteristic plume radius is given by

$$b = 0.42\left[\left(c_p\rho_\infty\right)^{4/5} T_\infty^{3/5} g^{2/5}\right]^{-1/2} \frac{T_p^{1/2}\dot{Q}_c^{2/5}}{\Delta T_p^{3/5}} \tag{14.18}$$

The Heskestad and Hamada [6] correlation is derived from measurements made with propane burner fires having heat release rates from 12 to 764 kW and beneath ceilings up to 2.5 m in height. This correlation is found to be accurate for ratios of free flame height to ceiling height less than or equal to about 2.0. At greater flame-height ratios, significant heat released in the ceiling jet itself appears to be the cause for a lack of agreement with the correlation.

Flame Lengths in the Ceiling Jet It is very interesting to note an often-overlooked finding of Heskestad and Hamada [6]. When there is flame impingement on the ceiling (flame-height ratio >1), the mean flame radius along the ceiling from the plume centerline is observed to be about equal to the difference between the free flame height and the ceiling height. Hence, Heskestad and Hamada find that the total average length of flame from the burning fuel to the flame tip under the ceiling is virtually the same as the free flame height.

In an earlier study involving small (0.36–8 kW) pool fires beneath ceilings up to 0.336 m in height, Yu (You)[2] and Faeth [10] measure the mean flame radius along the ceiling. Their results yield a flame radius about one-half the difference between the free flame height and the ceiling height, or one-half that of Heskestad and Hamada, perhaps due to the smaller scale of their experiment.

Ceiling Jet Thickness For strong plumes, Atkinson and Drysdale [20] demonstrate that much of the plume kinetic energy is lost (possibly 75 % of that in the incident plume) during the process of ceiling impingement. As a result of this kinetic energy loss, the initial ceiling jet thickness after the turning region may be twice that expected for the case of weak plumes, about 11 % of the ceiling height at $r/H = 0.2$. Measurements made by Atkinson and Drysdale and by Yu [5] show that the ceiling jet thickness may reach a minimum of 8 % of ceiling height at $r/H = 0.5$ and then increase up to 12 % of ceiling height at large radial distances, as for weak plumes.

[2] H. Z. Yu formerly published under the spelling *You*.

Convective Heat Transfer to Horizontal Unconfined Ceilings

Convection is the dominant mode of heat transfer for the case of weak plumes impinging on ceilings. This heat-transfer regime is important for the prediction of activation times for detection devices and the prediction of damage for objects, such as cables or pipes, suspended below the ceiling. However, damage to the ceiling structure itself will much more likely be the result of strong plume (flame) impingement, for which heat transfer due to thermal radiation will be just as important or more important than convection [21]. The maximum convective heat flux to a ceiling occurs when the ceiling surface is at or near ambient temperature, T_∞, before there has been any significant heating of the ceiling material. This maximum convective flux is the subject of the following discussion. For additional discussion of ceiling heat loss, see Chap. 25.

Weak Plume Impingement (Turning) Region

Quantification of convective heat transfer from weak fire plumes impinging on ceiling surfaces has been an area of research activity for many years. In the turning region, a widely used correlation is derived by Yu and Faeth [10] from experiments with small pool fires (convective heat release rates, $\dot{Q}_c$, from 0.05 to 3.46 kW; ceiling heights, H, less than 1 m). This correlation gives convective heat flux to the ceiling, $\dot{q}''$, as

$$\frac{\dot{q}'' H^2}{\dot{Q}_c} = \frac{31.2}{\mathrm{Pr}^{3/5}\mathrm{Ra}^{1/6}} = \frac{38.6}{\mathrm{Ra}^{1/6}} \qquad (14.19)$$

where Pr is the Prandtl number, and the plume Rayleigh number, Ra, is given by

$$\mathrm{Ra} = \frac{g\dot{Q}_c H^2}{3.5 p \nu^3} = \frac{0.027\dot{Q}_c H^2}{\nu^3} \qquad (14.20)$$

for gases similar to air, having ambient absolute pressure, p, and kinematic viscosity, ν. It is recommended that when these expressions are applied to actual heat-transfer problems, the ceiling height should be corrected for the location of the virtual point source for the plume.

Note that the heat-flux parameter on the left side of Equation 14.19 is proportional to the classic heat-transfer Stanton number and that the Rayleigh number is proportional to the cube of the plume Reynolds number, Re (defined in terms of centerline velocity, characteristic plume diameter, $2b$, and kinematic viscosity at the plume centerline temperature).

Equation 14.19 has been established for mainly weak plumes with Rayleigh numbers from 10^9 to 10^{15}. Kokkala [22] has verified this impingement zone heat-transfer correlation, using up to 10 kW natural gas flames, for flame heights up to 70 % of the ceiling height. For greater flame height to ceiling height ratios, Kokkala [22] finds that heat-transfer rates are many times higher than predicted, partly due to thermal radiation.

Alpert [23] performed small-scale (0.3 m ceiling height) experiments at elevated air pressures, which allow Rayleigh numbers greater than 2×10^{15} to be achieved while maintaining somewhat better control of ambient disturbances than in 1-atm experiments. Results of these experiments essentially confirm the predictions of the correlation in Equation 14.19, as well as an expression recommended for the plume impingement region by Cooper [8]. The latter expression yields nondimensional ceiling heat transfer, in terms of the plume Reynolds number defined by Alpert [23], as follows:

$$\frac{\dot{q}'' H^2}{\dot{Q}_c} = 49 \times \mathrm{Re}^{-1/2} = 105\left(\frac{\dot{Q}_c^{1/3} H^{2/3}}{\nu}\right)^{-1/2} \qquad (14.21)$$

Although Equations 14.19 and 14.21 have identical dependence of impingement heat flux on fire heat release rate and ceiling height, heat-flux values from Equation 14.21 are about 50 % higher, since this expression is derived from data on turbulent jets.

Ceiling Jet Region

Outside of the turning region, the convective flux to the ceiling is known to drop off sharply with increasing radial distance from the plume axis. The experiments of Yu and Faeth [10] described in the preceding section were also used to determine this radial variation in ceiling jet convective flux. Their own data, as well as data from small-scale experiments (ceiling heights of 0.5 to 0.8 m) by Alpert [13] and by Veldman [11] are all consistent with the following correlation that is given by Yu and Faeth [10][3]:

$$\frac{\dot{q}'' H^2}{\dot{Q}_c} = 0.04\left(\frac{r}{H}\right)^{-1/3} \quad \text{for } 0.2 \le \frac{r}{H} < 2.0 \tag{14.22}$$

An alternate derivation of Equation 14.22 can be obtained by using Alpert's correlation for ceiling jet excess temperature (Equation 14.3) and Alpert's theory for average ceiling jet velocity (Equation 14.14) with the Reynolds/Colburn analogy, as discussed by Yu and Faeth [10] and Veldman [11]. From the Reynolds/Colburn analogy, the heat-transfer coefficient at the ceiling, h, should be related to ceiling jet average velocity and density as follows:

$$\frac{h}{\rho_\infty U c_p} = \mathrm{Pr}^{-2/3}\frac{f}{2} \tag{14.23}$$

where Pr is the Prandtl number and f is the ceiling friction factor. By using Equation 14.14 for average ceiling jet velocity, U, the ceiling heat-transfer coefficient becomes

$$h = 0.246 f \left(\frac{\dot{Q}_c}{H}\right)^{1/3}\left(\frac{r}{H}\right)^{-0.69} \quad \text{for } 0.17 \le \frac{r}{H} < 4.0 \tag{14.24}$$

With $f = 0.03$, Equation 14.24 is identical to the simplified expression listed in Beyler's extensive compilation [19]. The nondimensional heat flux to a ceiling at ambient temperature can then be expressed as follows, since $\dot{q}'' = h\Delta T$, with ΔT given by Equation 14.3:

$$\frac{\dot{q}'' H^2}{\dot{Q}_c} = 1.323 f \left(\frac{r}{H}\right)^{-1.36} \quad \text{for } 0.2 \le \frac{r}{H} < 4.0 \tag{14.25}$$

Equations 14.22 and 14.25 are in good agreement for a friction factor of 0.03, which is comparable with the value of 0.02 deduced from Alpert's [4] theory.

Sloped Ceilings

There have been very few studies of the ceiling jet flow resulting from plume impingement on an inclined, flat ceiling, i.e., where the ceiling is inclined at some angle, θ, to the horizontal. One such study, by Kung et al. [24], obtained measurements showing pronounced effects in the velocity variation along the steepest run from the point of impingement of a strong plume, both in the upward and downward directions. In the upward direction, the rate of velocity decrease with distance, r, from the intersection of the plume vertical axis with the ceiling was reduced significantly as the ceiling slope increased. In the downward direction, the flow separated from the ceiling and turned upward at a location, $-r$, denoted by Kung et al. [24] as the penetration distance. These results were the outcome of experiments with 0.15- and 0.228-m-diameter pan fires located 0.279 to 0.889 m beneath an inclined 2.4-m square ceiling and were limited to convective heat release rates in the range of 3–13 kW.

Following Heskestad and Hamada [6], Kung et al. developed correlations by scaling near-maximum excess temperature and velocity, as well as radial distance along the ceiling, in terms of the quantities in the undeflected plume at the impingement point. These correlations take the following form:

$$\frac{\Delta T}{\Delta T_p} = \exp\left[(0.12\sin\theta - 0.42)\left(\frac{r}{b} - 1\right)^{0.7}\right] \tag{14.26}$$

[3] Note that there is a typographical error in the exponent of r/H in Equation 14.17 of this reference.

$$\frac{U}{V_p} = \exp\left[(0.79\sin\theta - 0.52)\left(\frac{r}{b} - 1\right)^{0.6}\right] \tag{14.27}$$

for $r/b \geq 1$(upward direction from the impingement point, i.e., r = r_{up}) and θ = 0 − 30°;

$$\frac{\Delta T}{\Delta T_p} = (0.15\sin\theta - 0.11)\left(\frac{r}{b}\right) + 0.97 - 0.06\sin\theta \tag{14.28}$$

$$\frac{U}{V_p} = (0.21\sin\theta - 0.10)\left(\frac{r}{b}\right) + 0.99 - 1.17\sin\theta \tag{14.29}$$

for $r/b < 0$ (downward direction from the impingement point), valid only for θ = 0 − 30°, and for ΔT and U ≥ 0.

In Equations 14.26, 14.27, 14.28, and 14.29, the characteristic plume radius is proportional to that defined in Equation 14.18 but with a slightly different magnitude, namely,

$$b = 0.548\left[\left(c_p\rho_\infty\right)^{4/5}T_\infty^{3/5}g^{2/5}\right]^{-1/2}\frac{T_p^{1/2}\dot{Q}_c^{2/5}}{\Delta T_p^{3/5}} \tag{14.30}$$

Equation 14.29 shows that the ceiling jet velocity first becomes zero in the downward direction at values of r/b equal to −5.6, −3.5, and −2.0 for ceiling slopes of 10°, 20°, and 30°, respectively.

About 10 years after the work by Kung et al., additional measurements of gas temperature and velocity under inclined ceilings with thermocouples and bidirectional tubes, respectively, were obtained by Sugawa et al. [25]. These experiments involved nearly full-scale conditions (ceiling clearance, H, on the fuel centerline of 1.25–2.5 m) with a 200 mm diameter propane gas burner fire providing 10–100 kW heat release rates. Formulas for ceiling jet excess temperature and velocity along the "upslope" and perpendicular to the "upslope" directions are provided for slope angles from 0° to 60°. In many of these experiments, there is flame impingement on the ceiling and flame in the ceiling jet.

Very recently (about 10 years after the preceding studies by Sugawa et al.), new correlations have been developed by Y. Oka and colleagues at Yokohama National University from significant additional measurements under ceilings inclined from the horizontal up to a maximum angle, θ, of 40° and having a centerline clearance, H, above the fuel surface of 1 m. In these studies [26, 27], ceiling jet gas velocity is measured not only with bi-directional tubes but also with a Particle Imaging Velocimetry (PIV) system that makes use of smoke particles naturally present in the plume from the 0.285 m square heptane pan fire (heat release rate of 43 kW). By having two methods for measuring velocity, the authors [26] determined that the bidirectional probe generally provided a bulk mean velocity whereas the high resolution PIV system could provide a true maximum velocity. The ratio of the former to the latter is determined to be 0.828 instead of 0.707, as would be expected for the classic half-Gaussian velocity profile. Algebraic expressions for ceiling jet velocity have been obtained [26] both for the case of the flame tip below the inclined ceiling and for flame impingement on the inclined ceiling. In the latter case, gas velocity continues to increase in the flame zone in the steepest upward direction from the impingement point (as occurs in the fire plume itself) before becoming nearly constant and then decreasing with distance in the upward direction. Oka et al. [27] have now developed, from data for $0 < \theta < 40°$, a single algebraic expression for maximum ceiling jet gas velocity, U_{up}, at the steepest upward radial distance, r_{up}, from plume impingement, which covers cases both with and without flame impingement on a ceiling, as follows:

$$\frac{U_{up}}{\sqrt{g\left(H + r_{up}\sin\theta\right)}} = \alpha\left[\frac{r_{up}\cos\theta}{H + r_{up}\sin\theta}\right]^{\beta}\left\{Q_c^*(1 + \sin\theta)\right\}^{1/3} \tag{14.31}$$

where, for

$$\begin{array}{lll} 0.037 < r_{\text{up}} \cos\theta / \left(H + r_{\text{up}} \sin\theta\right) \leq 0.151 & \alpha = 6.051, & \beta = 0.458 \\ 0.151 < r_{\text{up}} \cos\theta / \left(H + r_{\text{up}} \sin\theta\right) \leq 0.350 & \alpha = 2.540, & \beta = 0 \\ 0.350 < r_{\text{up}} \cos\theta / \left(H + r_{\text{up}} \sin\theta\right) \leq 1.80 & \alpha = 0.855, & \beta = -1.040 \end{array}$$

and $Q_c^* =$ the usual definition (see Equation 14.9) with $\dot{Q}$ the convective component of heat release rate

The corresponding algebraic expression for near-maximum excess ceiling jet gas temperature from extensive thermocouple measurements that covers cases both with and without flame impingement on the ceiling is given by the following:

$$\frac{\Delta T}{T_\infty} = 2.778 \left[\frac{r_{up} \cos\theta}{H}\right]^{-0.781} \left\{Q_c^* (1 + \sin\theta)\right\}^{2/3} \quad 0.1 \leq r_{up} \cos\theta / H \leq 2.4 \tag{14.32}$$

The detailed velocity and excess temperature measurements discussed above have allowed Oka et al. [26] also to derive algebraic expressions for Gaussian ceiling jet velocity and excess temperature thickness under sloped ceilings. They determined that ceiling jet thickness was not affected by flame impingement as long as data corresponding to any region of continuous flaming are excluded. The expression for Gaussian thermal thickness under a sloped ceiling is given by:

$$\frac{L_T}{H} = \{0.00254\theta + 0.112\}\left[1 - exp\left(\beta_T \frac{r_{up}}{H}\right)\right] \tag{14.33}$$

where $\beta_T = -2.91 + 2.20[1 - \exp(-0.0662\theta)]$ and valid for $0.4 \leq r_{up}/H \leq 2.4$; $0 \leq \theta \leq 40°$.

Time-Dependent Fires

Quasi-Steady Assumption

For time-dependent fires, all estimates from the previous section may still be used, but with the constant heat release rate, $\dot{Q}$, replaced by an appropriate time-dependent $\dot{Q}(t)$. In making this replacement, a "quasi-steady" flow has been assumed. This assumption implies that when a change in heat release rate occurs at the fire source, full effects of the change are immediately felt everywhere in the flow field. In a room-sized enclosure, under conditions where the fire is growing slowly, this assumption is reasonable. However, in other cases, the time for the heat release rate to change significantly may be comparable to or less than the time, $t_f - t_i$, for gas to travel from the burning fuel to a detector submerged in the ceiling jet. The quasi-steady assumption may not be appropriate in this situation, unless the following condition is satisfied, depending on the accuracy desired:

$$\frac{\dot{Q}}{d\dot{Q}/dt} > t_f - t_i \tag{14.34}$$

where t_i is an ignition reference time.

The quasi-steady assumption, together with the strong plume-driven ceiling jet analysis of Heskestad and Hamada [6], has been used by Kung et al. [28] to correlate ceiling jet velocity and temperature induced by growing rack-storage fires. Although gas travel times for these large-scale experiments may amount to many seconds, Equation 14.34 shows that a sufficiently small fire-growth rate allows a quasi-steady analysis to be used.

Testing has shown that the heat release rate during the growth phase of many fires can often be characterized by simple time-dependent polynomial or exponential functions. The most extensive research and analysis have been performed with heat release rates that vary with the second power of time.

Power-Law Fire Growth

The growth phase of many fires can be characterized by a heat release rate increasing proportionally with a power, p, of time measured from the ignition reference time, t_i, as follows:

$$\dot{Q} = \alpha(t - t_i)^p \tag{14.35}$$

Figure 14.5 shows one case where the heat release rate for a burning foam sofa during the growth phase of the fire, more than 80 s (t_i) after ignition [29], can be represented by the following equation:

$$\dot{Q} = 0.1736(t - 80)^2 \tag{14.36}$$

Heskestad [30] used the general power-law behavior given by Equation 14.35 to propose a set of theoretical modeling relations for the transient ceiling jet flow that would result from such a time-varying heat release rate. These relations were validated in an extensive series of tests conducted by Factory Mutual Research Corporation [18, 31], where measurements were made of maximum ceiling jet temperatures and velocities during the growth of fires in three different sizes of wood crib. Subsequent to this original experimental study, Heskestad and Delichatsios [32] corrected the heat release rate, $\dot{Q}$, computed for the crib tests and also generalized their results to other types of fuels by using the more relevant convective heat release rate, $\dot{Q}_c$. The resulting dimensionless correlations for maximum ceiling jet temperatures and velocities are given by

$$\Delta T_2^* = 0 \quad t_2^* \le \left(t_2^*\right)_f \tag{14.37}$$

$$\Delta T_2^* = \left(\frac{t_2^* - \left(t_2^*\right)_f}{0.126 + 0.210r/H}\right)^{4/3} \quad t_2^* > \left(t_2^*\right)_f \tag{14.38}$$

$$\frac{U_2^*}{\sqrt{\Delta T_2^*}} = 0.59\left(\frac{r}{H}\right)^{-0.63} \tag{14.39}$$

where

$$t_2^* = \frac{t - t_i}{\left(A\alpha_c H^{-4}\right)^{-1/5}} \tag{14.40}$$

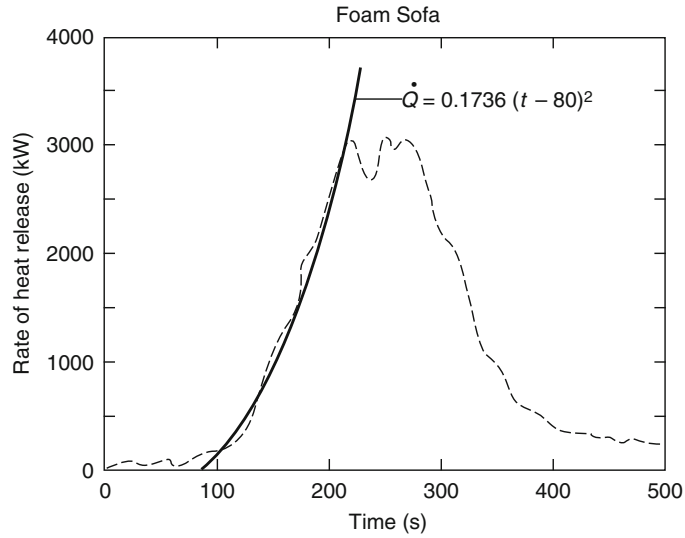

Fig. 14.5 Heat release rate history for a burning foam sofa [29]

$$U_2^* = \frac{U}{(A\alpha_c H)^{1/5}} \tag{14.41}$$

$$\Delta T_2^* = \frac{(T - T_\infty)/T_\infty}{(A\alpha_c)^{2/5} g^{-1} H^{-3/5}} \tag{14.42}$$

$$A = \frac{g}{\rho_\infty c_p T_\infty} \tag{14.43}$$

$$\alpha_c = \frac{\dot{Q}_c}{(t - t_i)^2} \tag{14.44}$$

$$(t_2^*)_f = 0.813\left(1 + \frac{r}{H}\right) \tag{14.45}$$

and where dimensionless variables are indicated with the superscript asterisk.

Notice that in Equation 14.38 the dimensionless time, t_2^*, has been reduced by the time $(t_2^*)_f$. This reduction accounts for the gas travel time, $t_f - t_i$, between the fire source and the location of interest along the ceiling at the specified r/H. For dimensionless times after ignition less than $(t_2^*)_f$, the initial heat front has not yet arrived at r/H so the gas temperature is still at the ambient value, as shown in Equation 14.37. In dimensional terms, the gas travel time is given by the following, after using the definition of t_2^* in Equation 14.45:

$$t_f - t_i = H^{4/5} \frac{0.813(1 + r/H)}{(A\alpha_c)^{1/5}} \tag{14.46}$$

Substitution of Equation 14.35 into Equation 14.34 shows that for power-law fire growth, the quasi-steady assumption will always be valid beginning at a sufficiently long time after ignition. For the specific case of t^2 fire growth, substitution of Equation 14.44 and the expression for the gas travel time, Equation 14.46, into Equation 14.34 results in the following requirement if a quasi-steady analysis is to be appropriate:

$$\frac{t - t_i}{2} > H^{4/5} \frac{0.813(1 + r/H)}{(A\alpha_c)^{1/5}} \tag{14.47}$$

In the limit of very large values of $t - t_i$, Equation 14.47 will always be satisfied and a quasi-steady limit is achieved, as shown by an alternative method by Heskestad [18]. The value of the quasi-steady excess temperature, $(\Delta T_2^*)_{qs}$, in this limit of $t_2^* \gg (t_2^*)_f$ becomes, from Equation 14.38

$$(\Delta T_2^*)_{qs} = \left(\frac{t_2^*}{0.126 + 0.210 r/H}\right)^{4/3} \tag{14.48}$$

The preceding correlations of ceiling jet temperatures and velocities are the basis for the calculated values of fire detector spacing found in *NFPA 72®*, *National Fire Alarm Code®*, Appendix B, "Engineering Guide for Automatic Fire Detector Spacing" [33]. In *NFPA 72*, three or four selected fire heat release rates assumed to increase proportionally with the square of time are used as the basis for the evaluation. These fire heat release rate histories are chosen to be representative of actual fires involving different commodities and geometric storage arrangements. The chosen release rate histories are as follows:

$$\text{Slow} \qquad \dot{Q} = 0.00293 t^2 \tag{14.49}$$

$$\text{Medium} \qquad \dot{Q} = 0.01172 t^2 \tag{14.50}$$

$$\text{Fast} \qquad \dot{Q} = 0.0469 t^2 \tag{14.51}$$

$$\text{Ultrafast} \qquad \dot{Q} = 0.1876 t^2 \tag{14.52}$$

where $\dot{Q}$ is in kW and t is in s.

EXAMPLE Sofa fire: Consider how the following calculation demonstrates a use of the correlation (Equations 14.38 and 14.39) for calculating the ceiling jet maximum temperature and velocity produced by a t^2 fire growth.

A foam sofa, of the type analyzed in Fig. 14.5, is burning in a showroom 5 m below a suspended ceiling. The showroom temperature remote from the fire remains at 20 °C at floor level as the fire begins to grow. Determine the gas temperature and velocity at the position of a ceiling-mounted fire detector submerged in the ceiling jet flow 4 m away from the fire axis when the convective heat release rate (assumed to equal the total heat release rate) first reaches 2.5 MW.

Figure 14.5 shows that the heat release rate from the sofa first reaches 2.5 MW (2500 kW) at about 200 s after ignition. Using the analytic formula for the time-dependent heat release rate, Equation 14.36, the time from the virtual ignition of the sofa at 80 s to reach 2500 kW is

$$2500 - 0.1736(t - 80)^2$$
$$(t - 80) = 120 \text{ s}$$

In this problem, the low-level heat release rate up to 80 s after actual ignition of the sofa is ignored. Thus, the sofa fire can be treated as having started at $t = 80$ s and grown to 2.5 MW in the following 120 s. Equations 14.40, 14.41, 14.42, 14.43, 14.44, and 14.45 are used to evaluate parameters of the problem, using the dimensionless correlations for ceiling jet temperature and velocity.

For the sofa fire in the showroom example, $T_\infty = 293$ K, $\rho = 1.204$ kg/m^3, $c_p = 1$ kJ/kg·K, $g = 9.8$ m/s^2, $\alpha_c = 0.1736$ kW/s^2, $A = 0.0278$ m^4/kJ · s^2, $r = 4$ m, $H = 5$ m, $\left(t_2^*\right)_f = 1.46$, $t - t_i = 120$ s, and $t_2^* = 11.40$. For the conditions of interest, $t_2^* > \left(t_2^*\right)_f$, so the correlation (Equation 14.38) is used to evaluate the dimensionless ceiling jet temperature

$$\Delta T_2^* = \left[\frac{11.40 - 1.46}{0.126 + 0.210(4/5)}\right]^{4/3}$$
$$\Delta T_2^* = 109.3$$

Equation 14.39 is used to calculate the dimensionless ceiling jet velocity

$$U_2^* = 0.59(4/5)^{-0.63}\sqrt{109.3} = 7.10$$

The dimensional excess temperature and velocity are calculated using Equations 14.42 and 14.41, respectively, to yield

$$\Delta T = 147\,\text{K}$$
$$T = 147\,\text{K} + 293\,\text{K} = 440\,\text{K} = 167^\circ\text{C}$$
$$U = 3.37\,\text{m/s}$$

The corresponding gas temperature calculated with the quasi-steady analysis of Equation 14.48 instead of the fire analysis is 197 °C.

EXAMPLE Rack storage: Yu and Stavrianidis [34] were interested in predicting activation times of quick-response sprinklers protecting high rack storage of plastics. Since the sprinklers are activated typically in less than 1 min by the ceiling jet flow, information on flow temperature and velocity shortly after ignition is required. The objective was to correlate properties of the ceiling jet induced by fires in 2- to 5-tier-high rack storage, consisting of polystyrene cups packaged in corrugated paper cartons on pallets. When this fuel array is ignited at its base, the initial growth period ($t_f - t_i \approx 25$ s) can be characterized as heat release rates increasing by the third power of time, as follows:

$$\dot{Q}_c = \alpha_c (t - t_i)^3 \tag{14.53}$$

where $\alpha_c = 0.0448$. Because of upward and lateral flame propagation during the transient rack-storage fire, the virtual origin elevation, z_o, of the plume changes during the course of fire growth, as follows:

$$z_o = -2.4 + 0.095\dot{Q}_c^{2/5} \tag{14.54}$$

thereby complicating the effort to correlate ceiling jet properties. Nevertheless, Yu and Stavrianidis were able to develop correlations based on the following dimensional temperature and velocity variables, which are similar to those first proposed by Heskestad [30] for power-law fire growth:

$$\Delta\hat{T}_m = \alpha_c^{-1/3}(H - z_o)^{1/3}\frac{\Delta T_m}{T_\infty} \tag{14.55}$$

$$\hat{U}_m = \alpha_c^{-1/6}(H - z_o)^{-1/3}U_m \tag{14.56}$$

where the maximum ceiling jet excess temperature, $\Delta\hat{T}_m$, and velocity, $\hat{U}_m$, variables depend on the following heat release rate and radial distance parameters, respectively:

$$X = \alpha_c^{-1/6}(H - z_o)^{-2/3}\dot{Q}_c^{1/3} \tag{14.57}$$

$$\hat{R} = \frac{r}{H - z_o} \tag{14.58}$$

The exact form of the preceding correlations, in terms of detailed formulas, is provided by Yu and Stavrianidis [34].

In addition to maximum excess gas temperature and velocity, Yu and Stavrianidis [34] also measured the depth of the ceiling jet, in terms of the distance below the ceiling where the velocity and excess temperature are $1/e$ of the respective maximum values. Results show the ceiling jet depth based on velocity to be very similar to that based on excess temperature and both depths to be fairly insensitive to the transient fire growth process. Typical values for the ratio of ceiling jet temperature depth to effective ceiling height, $\ell_T/(H - z_o)$, for radial positions, $r/(H - z_o)$ of 0.217, 0.365, 1.75, and 4.33 are about 0.07, 0.1, 0.14, and 0.2, respectively.

Confined Ceilings

Channel Configuration

Previous discussions of ceiling jets in this chapter have all dealt with unconfined radial spread of the gas flow away from a ceiling impingement point. In practice this flow may be interrupted by ceiling beams or corridor walls, creating a long channel that partially confines the flow. Knowledge of the resultant ceiling jet flows is important in determining fire detector response times. For the channel configuration, the flow near the impingement point will remain radial (i.e., axisymmetric), but after spreading to the walls or beams that bound the ceiling, the flow will become generally parallel with the confining boundary. Delichatsios [35] has developed correlations for steady-state ceiling jet temperature and velocity, which apply to the channel flow between beams and down corridors. In the case of corridors, the correlations apply when the corridor half-width, ℓ_b, is greater than 0.2 times the ceiling height, H, above the fire source. Note that this value of ℓ_b corresponds approximately to the outer radius of the ceiling jet turning region. In the case of beams, the flow must also be contained fully so that only a flow in a primary channel results, without spillage under the beams to the adjoining secondary channels. For the latter condition to be satisfied, the beam depth, h_b, must be greater than the quantity $(H/10)(\ell_b/H)^{-1/3}$. Downstream of where the ceiling jet flow is parallel to the beams or corridor walls and in the absence of spillage, Delichatsios [35] determined that the average excess ceiling jet temperature and velocity within the primary channel are given by the following:

$$\frac{\Delta T}{\Delta T_p} = \mathrm{a}\left(\frac{H}{\ell_b}\right)^{1/3} \exp\left[-6.67\mathrm{St}\frac{Y}{H}\left(\frac{\ell_b}{H}\right)^{1/3}\right] \tag{14.59}$$

$$U = 1.102\sqrt{H\Delta T}\left(\frac{H}{\ell_b}\right)^{1/6} \tag{14.60}$$

under the conditions

$$Y > \ell_b$$
$$h_b/H > 0.1(\ell_b/H)^{-1/3}$$
$$\ell_b/H > 0.2$$
$$0.5 < \frac{Y}{H}\left(\frac{\ell_b}{H}\right)^{1/3} < 3.0$$

where

ΔT_p = Excess temperature on the plume centerline defined previously in Equation 14.17

Y = Distance along the channel measured from the plume impingement point

St = Stanton number, whose value is recommended to be 0.03

Based on the minimum value of $\ell_b/H = 0.2$, the limit on h_b/H implies that the beam depth to ceiling height ratio must be at least 0.17 for the fire gases to be restricted to the primary channel. The constant a in Equation 14.59 is determined by Delichatsios to be in the range 0.24–0.29. This equation is based on the concept that the channel flow has undergone a hydraulic jump, which results in greatly reduced entrainment of cooler, ambient air from below. Reductions in ceiling jet temperature or velocity are then mainly due to heat losses to the ceiling and would thus be dependent on ceiling composition to some extent.

Additional detailed measurements of the ceiling jet flow in a primary beamed channel have been obtained by Koslowski and Motevalli [36]. Their data generally validate the

Delichatsios beamed ceiling correlation (Equation 14.61) and ceiling jet flow behavior, but additional measurements for a range of beam depth to ceiling height ratios has allowed the correlation to be generalized. Furthermore, Koslowski and Motevalli recast the correlation in terms of the nondimensional heat release rate defined by Heskestad and Delichatsios (Equations 14.9 and 14.10), instead of centerline plume conditions at the ceiling, with the following result:

$$\Delta T_0^* = \mathrm{C}\left(\frac{H}{\ell_b}\right)^{1/3} \exp\left[-6.67\,\mathrm{St}\frac{Y}{H}\left(\frac{\ell_b}{H}\right)^{1/3}\right] \tag{14.61}$$

where the Stanton number is recommended to be 0.04, rather than 0.03, and the constant, C, has the following dependence on the ratio of beam depth, h_b, to ceiling height, H:

$$\mathrm{C} = -25.38\left(\frac{h_b}{H}\right)^2 + 13.58\frac{h_b}{H} + 2.01 \quad \text{for } 0.5 \le \frac{Y}{H} \le 1.6 \tag{14.62}$$

To derive Equation 14.62, Koslowski and Motevalli vary the h_b/H ratio from 0.07 up to 0.28. In so doing, they note that C increases steadily with this ratio until leveling off near $h_b/H = 0.17$, determined by Delichatsios as the condition for the fire gases to be restricted to the primary channel. Between values of h_b/H of 0.07 (or even much less) and 0.17, spillage from the primary channel to adjacent secondary channels is steadily reduced, thereby increasing temperatures in the primary channel. Characteristics of the ceiling jet flow in the secondary channels, as well as the primary channel, have also been studied by Koslowski and Motevalli [37].

Corner Configuration with Strong Plumes

An open configuration of two walls at a 90° angle to form a corner, covered by a ceiling, with a fire source at the base of and in close contact with the corner, is often used as a hazardous environment in which to test the flammability of wall and ceiling linings. This wall-ceiling-corner configuration also occurs naturally in many types of enclosures (see below) where hot gases from the fire source may be partially or completely confined by more than just the ceiling and corner walls themselves, resulting in the formation of a hot gas layer near the ceiling. In this section, the environment of an open corner with inert lining surfaces is discussed, where a ceiling jet develops due to impingement of a fire plume or flames from the source fire at the base of the wall corner onto the ceiling covering the wall-corner. A careful study of this environment based on full-scale tests was conducted by Lattimer and Sorathia [38]. These tests used a ceiling clearance of 2.25 m above the surface of a 0.17–0.50 m^2 or L-shaped line (each leg being 0.17–0.50 m) sand burner having propane heat release rates from 50 to 300 kW.

Thermocouple measurements [38] of excess gas temperature at a radial distance from the corner, r, in the ceiling jet could be correlated (with a regression coefficient of 0.85) by the following formulas:

$$T - T_\infty = 950 \quad \text{for} \quad \frac{r+H}{L_{f,tip}} \le 0.55 \tag{14.63}$$

$$T - T_\infty = C\left[\frac{r+H}{L_{f,tip}}\right]^{-2} \quad \text{for} \quad \frac{r+H}{L_{f,tip}} > 0.55 \tag{14.64}$$

The specific value of 950 for the maximum excess of corner fire gas temperature above ambient in Equation 14.63 may vary for fire sources other than the propane burner or for corner walls having thermal characteristics different from those used in these specific tests. However, it is expected that the functional dependencies for ceiling jet temperature should be preserved. Note that the constant, C, in Equation 14.64 is 288 for the square burner of side, D, and 340 for the L-shaped line burner, each leg of which is length, D and that $L_{f,tip}$ is the flame length from the surface of either type burner to the flame tip, the furthest location where flame

tips are observed visually, as determined from the correlation [38],

$$\frac{L_{f,tip}}{D} = 5.9\sqrt{Q^*} \qquad (14.65)$$

where Q^* is based on actual fire heat release rate and the burner length-scale, D (instead of the usual ceiling clearance, H).

Lattimer and Sorathia [38] also used twenty Schmidt-Boelter gauges to measure heat flux to the bounding surfaces of the corner configuration from the propane sand burner flames. Their measurements of total heat flux, $\dot{q}''$, to the ceiling surface from the ceiling jet flames and/or hot gases could be correlated by the following for either the square or L-shaped line burner:

$$\dot{q}'' = 120 \quad \text{for} \quad \frac{r+H}{L_{f,tip}} \leq 0.58 \qquad (14.66)$$

$$\dot{q}'' = 18\left[\frac{r+H}{L_{f,tip}}\right]^{-3.5} \quad \text{for} \quad \frac{r+H}{L_{f,tip}} > 0.58 \qquad (14.67)$$

where the flame tip total length is given by Equation 14.65, above. This same formula is found also to predict the maximum heat flux to the top portion of the wall from the ceiling jet flow, where now the variable, r, represents distance from the corner along the top of the wall.

Again, the specific maximum heat flux of 120 kW/m^2 that was measured in the corner configuration by Lattimer and Sorathia [38] may vary for fuels with thermal radiation characteristics much different from those of propane or for different burner configurations. For example, it is well known that peak heat fluxes in pool and solid fuel fires can exceed 140–160 kW/m^2, as discussed by Coutts [39].

General Enclosure Configurations

The analyses in preceding sections for unconfined ceiling jet flows may be sufficient for large industrial or commercial storage facilities. In smaller rooms, or for very long times after fire ignition in larger industrial facilities, a quiescent, heated layer of gas will accumulate in the upper portion of the enclosure. This heated layer can be deep enough to totally submerge the ceiling jet flow. In this case, temperatures in the ceiling jet can be expected to be greater than if the ceiling jet were entraining gas from a cooler, ambient-temperature layer. It has been shown by Yu and Faeth [10] that the submerged ceiling jet also results roughly in a 35 % increase in the heat transfer rate to the ceiling.

There are analytical formulas to predict temperature and velocity in such a two-layer environment, in which the ceiling jet is contained in a heated upper layer and the fire is burning in a lower, cool layer. This type of prediction, which has been developed by Evans [40, 41], Cooper [42], and Zukoski and Kubota [43], can best be used to check the proper implementation of readily available numerical models (e.g., zone or field/CFD) of fire-induced flows in enclosures. An example of a zone model to predict activation of thermal detectors by a ceiling jet submerged in a heated layer is the algorithm developed by Davis [44]. This model, which assumes that thermally activated links are always located below the ceiling at the point of maximum ceiling jet temperature and velocity, is based partly on a model and thoroughly documented software developed by Cooper [45].

Formulas to predict the effect of the heated upper layer in an enclosure are based on the assumption that the ceiling jet results from a fire contained in a uniform environment at the heated upper-layer temperature. This substitute fire has a heat release rate, $\dot{Q}_2$, and location below the ceiling, H_2, differing from those of the real fire. Calculation of the substitute quantities $\dot{Q}_2$ and H_2, depends on the heat release rate and location of the real fire, as well as the depths and temperatures of the upper and lower layers within the enclosure.

Following the development by Evans [41], the substitute source heat release rate and distance below the ceiling are calculated from Equations 14.68, 14.69, 14.70, and 14.71. Originally developed for the purpose of sprinkler and heat detector response time calculations, these

equations are applicable during the growth phase of enclosure fires.

$$\dot{Q}^*_{I,2} = \left(\frac{1 + C_T \dot{Q}^{*\,2/3}_{I,1}}{\xi C_T} - \frac{1}{C_T} \right)^{3/2} \tag{14.68}$$

$$Z_{I,2} = \left\{ \frac{\xi \dot{Q}^*_{I,1} C_T}{\dot{Q}^{*\,1/3}_{I,2} \left[(\xi - 1)(\beta^2 + 1) + \xi C_T \dot{Q}^{*\,2/3}_{I,2} \right]} \right\}^{2/5} Z_{I,1} \tag{14.69}$$

$$\dot{Q}_{c,2} = \dot{Q}^*_{I,2} \rho_{\infty,2} c_{p\infty} T_{\infty,2} g^{1/2} Z^{5/2}_{I,2} \tag{14.70}$$

$$H_2 = H_1 - Z_{I,1} + Z_{I,2} \tag{14.71}$$

Further explanation of variables is contained in the nomenclature section.

Cooper [42] has formulated an alternative calculation of substitute source heat release rate and distance below the ceiling that provides for generalization to situations in which portions of the time-averaged plume flow in the lower layer are at temperatures below the upper-layer temperature. In these cases, only part of the plume flow may penetrate the upper layer sufficiently to impact on the ceiling. The remaining portion at low temperature may not penetrate into the hotter upper layer. In the extreme, when the maximum temperature in the lower-layer plume flow is less than the upper-layer temperature, none of the plume flow will penetrate significantly into the upper layer. This could be the case during the decay phases of an enclosure fire, when the heat release rate is small compared to earlier in the fire growth history. In this calculation of substitute fire-source quantities, the first step is to calculate the fraction of the plume mass flow penetrating the upper layer, m^*_2, from Equations 14.72 and 14.73.

$$m^*_2 = \frac{1.04599\sigma + 0.360391\sigma^2}{1 + 1.37748\sigma + 0.360391\sigma^2} \tag{14.72}$$

where

$$\sigma = \left(\frac{\xi}{\xi - 1} \right) \left[\frac{1 + C_T \left(\dot{Q}^*_{I,1} \right)^{2/3}}{\xi} - 1 \right] \tag{14.73}$$

Then, analogous to Equations 14.69, 14.70, and 14.71 of the previous method:

$$Z_{I,2} = Z_{I,1} \xi^{3/5} \left(m^*_2 \right)^{2/5} \left(\frac{1 + \sigma}{\sigma} \right)^{1/3} \tag{14.74}$$

$$\dot{Q}_{c,2} = \dot{Q}_{c,1} \left(\frac{\sigma m^*_2}{1 + \sigma} \right) \tag{14.75}$$

$$H_2 = H_1 - Z_{I,1} + Z_{I,2} \tag{14.76}$$

The last step is to use the substitute source values of heat release rate and distance below the ceiling, as well as heated upper-layer properties for ambient conditions, in the correlations developed for ceiling jet flows in uniform environments.

To demonstrate the use of the techniques, the previous example in which a sofa was imagined to be burning in a showroom may be expanded. Let all the parameters of the problem remain the same except that at 200 s after ignition ($t - t_i$ = 120 s), when the fire heat release rate has reached 2.5 MW, a quiescent heated layer of gas at a temperature of 50 °C is assumed to have accumulated under the ceiling to a depth of 2 m. For this case, the two-layer analysis is needed to determine the ceiling jet maximum temperature at the same position as calculated previously (a radial distance of 4 m from the plume impingement point on the ceiling).

All of the two-layer calculations presented assume quasi-steady conditions. From Equation 14.47 with the values of parameters in the single-layer calculation, it can be shown that the time after sofa ignition must be at least 31 s for a quasi-steady analysis to be acceptable. Since the actual time after ignition is 120 s, such an analysis is appropriate. It will be assumed that this finding will carry over to the two-layer case.

Using Equations 14.68, 14.69, 14.70, and 14.71 from the work of Evans [41], values of the heat release rate and position of the substitute fire source that compensates for the two-layer effects on the plume flow can be calculated. The dimensionless heat release rate of the real fire source evaluated at the position of the interface between the upper and lower layers is as follows:

$$\dot{Q}^*_{I,1} = \frac{\dot{Q}}{\rho_\infty c_{p\infty} T_\infty g^{1/2} Z^{5/2}_{I,1}} \qquad (14.77)$$

For an actual heat release rate of 2500 kW, ambient temperature of 293 K, and distance between the fire source and the interface between the lower and upper layers of 3 m, Equation 14.77 becomes

$$\dot{Q}^*_{I,1} = \frac{2500}{1.204 \times 1 \times 293 \times 9.8^{1/2} \times 3^{5/2}} = 0.1452$$

Using the ratio of upper-layer temperature to lower-layer temperature, $\xi = 323/293 = 1.1024$, and the constant, $C_T = 9.115$, the dimensionless heat release rate for the substitute fire source is

$$\dot{Q}^*_{I,2} = 0.1179$$

Using the value for the constant $\beta^2 = 0.913$, the position of the substitute fire source relative to the two-layer interface is

$$Z_{I,2} = 3.161$$

Now, from Equations 14.76 and 14.77, the dimensional heat release rate and position relative to the ceiling are found to be

$$\dot{Q}_2 = 2313\,\text{kW} \quad H_2 = 5.161\,\text{m}$$

The analogous calculations for substitute fire-source heat release rate and position following the analysis of Cooper [42], Equations 14.72, 14.73, 14.74, 14.75, 14.76, and 14.77, are

$$\sigma = 23.60$$
$$m^*_2 = 0.962$$
$$Z_{I,2} = 3.176$$
$$\dot{Q}_2 = 2308\,\text{kW}$$
$$H_2 = 5.176\,\text{m}$$

These two results are essentially identical for this type of analysis.

Since it has been shown that the quasi-steady analysis is appropriate for this example, the dimensionless maximum temperature in the ceiling jet flow, 4 m from the impingement point, can now be calculated from $(\Delta T_2{}^*)_{qs}$ in Equation 14.48. Using the ceiling height above the substitute source, this equation yields the result

$$\left(\Delta T^*_2\right)_{qs} = \left[\frac{11.40}{0.126 + 0.210(4/5.161)}\right]^{4/3} = 134.4$$

For the given time after ignition of 120 s and the assumed fire growth, the calculated $\dot{Q}_2$ value implies that α equals 0.1606, instead of the original sofa fire growth factor of 0.1736. Substitution of this new α in Equation 14.42, along with H_2 and the upper-layer temperature as the new ambient value, yields the following dimensional excess temperature at the 4-m radial position in the ceiling jet:

$$\Delta T = \frac{134.4 \times 323 \times (0.0278 \times .01606)^{2/5}}{9.8 \times 5.161^{3/5}}$$
$$\Delta T = 190\,\text{K}$$
$$T = 190\,\text{K} + 323\,\text{K} = 513\,\text{K} = 240^\circ\text{C}$$

This is 73 °C above the temperature calculated previously using the quasi-steady analysis and a uniform 20 °C ambient, demonstrating the effect of flow confinement on gas temperature.

Ceiling Jet Development

At the beginning of a fire, the initial buoyant flow from the fire must spread across the ceiling, driven by buoyancy, to penetrate the cooler ambient air ahead of the flow. Research studies designed to quantify the temperatures and velocities of this initial spreading flow have been initiated [46]. At a minimum, it is useful to become aware of the many fluid mechanical phenomena embodied in a description of the ceiling jet flow in a corridor up to the time when the ceiling jet is totally submerged in a quiescent, warm upper layer. Borrowing heavily from a description of this flow provided by Zukoski et al. [46], the process is as follows.

A fire starts in a small room with an open door to a long corridor having a small vent near the floor at the end opposite the door. As the fire

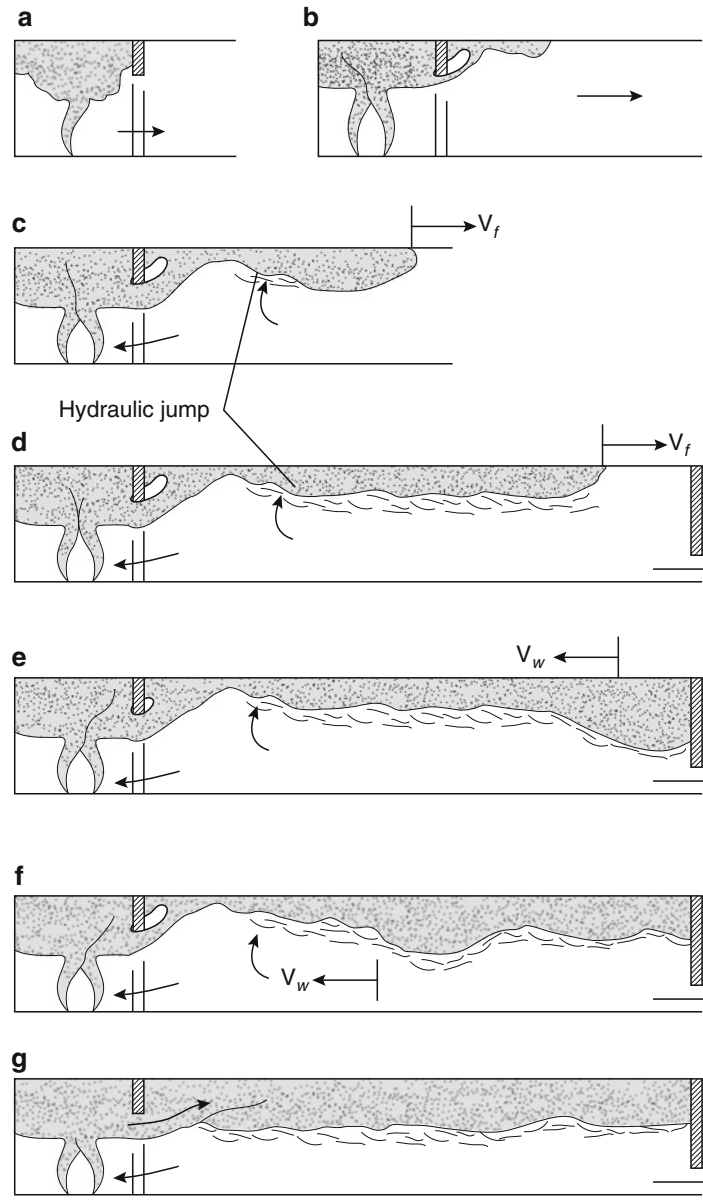

Fig. 14.6 Transient ceiling jet flow in a room and corridor [45]

starts, smoke and hot gases rise to form a layer near the fire room ceiling. The layer is contained in the small room by the door soffit (Fig. 14.6a). As the fire continues, hot gas from the room begins to spill out under the soffit into the hallway. The fire grows to a relatively constant heat release rate.

The outflowing gas forms a short, buoyant plume (Fig. 14.6b) that impinges on the hallway ceiling, producing a thin jet that flows away from the fire room in the same manner that the plume within the room flows over the interior ceiling. The gas flow in this jet is supercritical, analogous to the shooting flow of liquids over a weir. The velocity of the gas in this flow is greater than the speed of gravity waves on the interface between the hot gas and the cooler ambient air. The interaction of the leading edge of this flow with the ambient air ahead of it produces a hydraulic, jumplike condition, as shown in Fig. 14.6c.

A substantial amount of ambient air is entrained at this jump. Downstream of the jump, the velocity of the gas flow is reduced and mass flow is increased due to the entrainment at the jump. A head is formed at the leading edge of the flow. Mixing between this ceiling-layer flow and the ambient cooler air occurs behind this head.

The flow that is formed travels along the hallway ceiling (Fig. 14.6c, d) with constant velocity and depth until it impinges on the end wall (Fig. 14.6e). A group of waves are reflected back toward the jump near the fire room, traveling on the interface. Mixing occurs during the wall impingement process (Fig. 14.6f), but no significant entrainment occurs during the travel of the nonbreaking reflected wave. When these waves reach the jump near the fire room door, the jump is submerged in the warm gas layer, eliminating the entrainment of ambient lower-layer air at this position (Fig. 14.6g).

After several wave reflections up and down the corridor along the interface, the wave motion dies out, and a ceiling layer uniform in depth is produced. This layer slowly grows deeper as the hot gas continues to flow into the hallway from the fire room.

It is clear from the preceding description that quantification of effects during development of a submerged ceiling jet flow is quite complex.

Analyses and experiments have been performed to better understand the major features of a developing ceiling jet flow in a corridor [47, 48]. One such study [49] contains a description somewhat different from that already given.

Summary

Reliable formulas are available to predict maximum gas temperatures and velocities and approximate temperature/velocity profiles in fire-driven ceiling jet flows beneath unobstructed ceilings for both steady and power-law fire growth. These predictive formulas, which also apply to certain situations where the ceiling jet flow is confined by beams or corridor walls, are very useful for verifying that detailed numerical models of fire phenomena (e.g., Hara and Shinsuke [50]) have been implemented properly. The predictive techniques are the basis for acceptable design of fire detection systems, as exemplified by Appendix B of *NFPA 72®, National Fire Alarm Code* [33].

Nomenclature

A	$g/(\rho_\infty c_p T_\infty)(\mathrm{m}^2/\mathrm{kg})$
a	Constant in Equation 14.59, equal to 0.24–0.29
b	Effective plume radius at the intersection with the ceiling elevation (m)
C_T	Constant [17], related to plume flow, equal to 9.115
c_p	heat capacity at constant pressure (J/kg K)
D	Burner dimension (m)
D_{eff}	Effective diameter of the base of the flame zone or the burning fuel
f	Ceiling friction factor
g	Gravitational acceleration $(\mathrm{m/s}^2)$
H	Ceiling height above fire source; for sloped ceiling, on the fire axis (m)
h	Heat transfer coefficient $(\mathrm{kW/m}^2\ \mathrm{K})$
h_b	Depth of beams in a primary beam channel (m)
$L_{f,tip}$	Visible flame length from burner to furthest flame tip (m)
ℓ_b	Half-width for corridor or primary beam channel (m)
ℓ_T	Ceiling jet thickness based on $1/e$ depth of excess temperature profile (m)
m_2^*	Fraction of fire-plume mass flux penetrating upper layer
p	Ambient air pressure (Pa); also, as exponent of time for general power-law fire growth
Pr	Prandtl number
$\dot{Q}$	Total heat release rate (kW)
$\dot{Q}_c$	Convective heat release rate (kW)

$Q^*, \dot{Q}_0^*$	$\dot{Q}/\left(\rho_\infty c_p T_\infty \sqrt{g} H^{5/2}\right)$
Q_{fc}^*	$\dot{Q}_c/\left(\rho_\infty c_p T_\infty \sqrt{g} H^{5/2}\right)$
$\dot{q}''$	Rate of heat transfer per unit area (heat flux) to the ceiling surface (kW/m^2)
R	Radial distance to detector (m)
$\hat{R}$	$r/(H - z_o)$
Ra	Rayleigh number
Re	Reynolds number
r	Radial distance from axis of fire plume (m)
r_{up}	Radial distance in steepest upward direction from axis of fire plume (m)
St	Stanton number, $h/(\rho U c_p)$
T	Ceiling jet gas temperature (K)
T_∞	Ambient air temperature (K)
T_p	Peak gas temperature in plume at the intersection with ceiling elevation (K)
ΔT	Excess gas temperature, $T - T_\infty$ (K) or (°C)
t	Time (s)
U	Ceiling jet gas velocity (m/s)
U_{up}	Maximum ceiling jet gas velocity in the steepest upward direction (m/s)
V_p	Maximum plume velocity at the intersection with ceiling elevation (m/s)
Y	Distance along channel or corridor, measured from plume axis (m)
Z_I	Distance of layer interface above the real or substitute fire source (m)
z	Vertical distance above the base of the flame zone
z_H	Distance of ceiling above the base of the flame zone
z_o	Virtual origin elevation in a transient rack storage fire
z_v	Distance of virtual plume origin above the base of the flame zone
$d\dot{Q}/dt$	Rate of change of heat release rate with time (kW/s)

Greek Letters

α	Growth parameter for t^2 fires (kW/s^2)
β^2	Constant [17] related to plume flow, equal to 0.913
ν	Kinematic viscosity (m^2/s)
θ	Angle of inclination of the ceiling with respect to the horizontal (degrees)
ρ	Gas density (kg/m^3)
σ	Parameter defined in Equation 14.73
ξ	Ratio of temperatures, $T_{\infty,2}/T_{\infty,1}$

Subscripts

0	Based on steady-state fire source
1	Associated with lower layer
2	Associated with upper layer; or parameter associated with t^2 fire growth
∞	Ambient, outside ceiling jet or plume flows
c	Convective fraction
f	Associated with gas travel time delay
I	Value at the interface position between the heated upper layer and cool lower layer
i	Reference value at ignition
p	Associated with plume flow
qs	Quasi-steady flow condition

Superscripts

*	Dimensionless quantity
^	Quantity related to transient rack-storage fire

References

1. R.W. Pickard, D. Hird, and P. Nash, "The Thermal Testing of Heat-Sensitive Fire Detectors," *F.R. Note 247,* Building Research Establishment, Borehamwood, UK (1957).
2. P.H. Thomas, "The Distribution of Temperature and Velocity Due to Fires Beneath Ceilings," *F.R. Note 141,* Building Research Establishment, Borehamwood, UK (1955).
3. R.L. Alpert, "Calculation of Response Time of Ceiling-Mounted Fire Detectors," *Fire Technology,* 8, p. 181 (1972)
4. R.L. Alpert, "Turbulent Ceiling Jet Induced by Large-Scale Fires," *Combustion Science and Technology*, 11, 197 (1975)
5. H.Z. Yu (You), "An Investigation of Fire-Plume Impingement on a Horizontal Ceiling: 2-Impingement and Ceiling-Jet Regions," *Fire and Materials,* 9, 46 (1985)
6. G. Heskestad and T. Hamada, "Ceiling Jets of Strong Fire Plumes," *Fire Safety Journal,* 21, 69, (1993)

7. G. Heskestad, "Physical Modeling of Fire," *Journal of Fire & Flammability,* 6, p. 253 (1975).
8. L.Y. Cooper, "Heat Transfer from a Buoyant Plume to an Unconfined Ceiling," *Journal of Heat Transfer,* 104, p. 446 (1982).
9. L.Y. Cooper and A. Woodhouse, "The Buoyant Plume-Driven Adiabatic Ceiling Temperature Revisited," *Journal of Heat Transfer,* 108, p. 822 (1986).
10. H.Z. Yu (You) and G.M. Faeth, "Ceiling Heat Transfer during Fire Plume and Fire Impingement," *Fire and Materials*, 3, 140 (1979)
11. C.C. Veldman, T. Kubota, and E.E. Zukoski, "An Experimental Investigation of the Heat Transfer from a Buoyant Gas Plume to a Horizontal Ceiling—Part 1: Unobstructed Ceiling," *NBS-GCR-77–97,* National Bureau of Standards, Washington, DC (1977).
12. V. Motevalli and C.H. Marks, "Characterizing the Unconfined Ceiling Jet Under Steady-State Conditions: A Reassessment," *Fire Safety Science, Proceedings of the Third International Symposium* (G. Cox and B. Langford, eds.), Elsevier Applied Science, New York, p. 301 (1991).
13. R.L. Alpert, "Fire Induced Turbulent Ceiling-Jet," *Technical Report Serial No. 19722–2,* Factory Mutual Research Corporation, Norwood, MA, p. 35 (1971).
14. D.D. Evans and D.W. Stroup, "Methods to Calculate the Response Time of Heat and Smoke Detectors Installed Below Large Unobstructed Ceilings," *Fire Technology*, 22, 54 (1986).
15. R.L. Alpert, "The Fire Induced Ceiling-Jet Revisited," in The Science of Suppression, Proceedings of Fireseat 2011 at the National Museum of Scotland, 9 November 2011, The University of Edinburgh, Edinburgh, Scotland, pp. 1–21.
16. A. Tewarson, "Generation of Heat and Gaseous, Liquid and Solid Products in Fires," SFPE Handbook of Fire Protection Engineering, this volume, (p. 3–142 in 4th Edition).
17. E.E. Zukoski, T. Kubota, and B. Cetegen, "Entrainment in Fire Plumes," *Fire Safety Journal*, 3, 107 (1981)
18. G. Heskestad and M.A. Delichatsios, "The Initial Convective Flow in Fire," *17th International Symposium on Combustion,* Combustion Institute, Pittsburgh, PA (1978).
19. C.L. Beyler, "Fire Plumes and Ceiling Jets," *Fire Safety Journal,* 11, p. 53 (1986).
20. G.T. Atkinson and D.D. Drysdale, "Convective Heat Transfer from Fire Gases," *Fire Safety Journal,* 19, p. 217 (1992).
21. Y. Hasemi, S. Yokobayashi, T. Wakamatsu, and A. Ptchelintsev, "Fire Safety of Building Components Exposed to a Localized Fire: Scope and Experiments on Ceiling/Beam System Exposed to a Localized Fire," *AsiaFlam 95—1st International Conference,* Interscience Communications, Ltd., London, p. 351 (1995).
22. M.A. Kokkala, "Experimental Study of Heat Transfer to Ceiling from an Impinging Diffusion Flame," *Fire Safety Science, Proceedings of the Third International Symposium* (G. Cox and B. Langford, eds.), Elsevier Applied Science, New York, p. 261 (1991).
23. R.L. Alpert, "Convective Heat Transfer in the Impingement Region of a Buoyant Plume," *ASME Journal of Heat Transfer,* 109, p. 120 (1987).
24. H.C. Kung, R.D. Spaulding, and P. Stavrianidis, "Fire Induced Flow Under a Sloped Ceiling," *Fire Safety Science, Proceedings of the Third International Symposium* (G. Cox and B. Langford, eds.), Elsevier Applied Science, New York, p. 271 (1991).
25. O. Sugawa, T. Hosozawa, N. Nakamura, A. Itoh and Y. Matsubara, "Flow Behavior under Sloped Ceiling," in Fifteenth Meeting of UJNR Panel on Fire Research and Safety, NISTIR 6588, National Institute of Standards and Technology, Gaithersburg, MD USA, March 2000.
26. Y. Oka, M. Ando and K. Kamiya, "Ceiling Jet Flow Properties for Flames Impinging on an Inclined Ceiling," *Fire Safety Science, Proceedings of the Tenth International Symposium,* International Association for Fire Safety Science, London, 2012.
27. Y. Oka and M. Ando, "Temperature and Velocity Properties of a Ceiling Jet Impinging on an Unconfined Inclined Ceiling," accepted for publication in *Fire Safety Journal,* 2012.
28. H.C. Kung, H.Z. Yu (You), and R.D. Spaulding, "Ceiling Flows of Growing Rack Storage Fires," *21st Symposium (International) on Combustion,* Combustion Institute, Pittsburgh, PA, p. 121 (1986).
29. R.P. Schifilliti, *Use of Fire Plume Theory in the Design and Analysis of Fire Detector and Sprinkler Response,* Thesis, Worcester Polytechnic Institute, Worcester, MA (1986).
30. G. Heskestad, "Similarity Relations for the Initial Convective Flow Generated by Fire," *ASME Paper No. 72-WA/HT-17,* American Society of Mechanical Engineers, New York (1972).
31. G. Heskestad and M.A. Delichatsios, "Environments of Fire Detectors," *NBS-GCR-77-86* and *NBSGCR-77-95,* National Bureau of Standards, Washington, DC (1977).
32. G. Heskestad and M.A. Delichatsios, "Update: The Initial Convective Flow in Fire," Short Communication, *Fire Safety Journal,* 15, p. 471 (1989).
33. *NFPA 72®, National Fire Alarm Code®,* National Fire Protection Association, Quincy, MA (1999).
34. H.Z. Yu and P. Stavrianidis, "The Transient Ceiling Flows of Growing Rack Storage Fires," *Fire Safety Science, Proceedings of the Third International Symposium (*G. Cox and B. Langford, eds.), Elsevier Applied Science, New York, p. 281 (1991).
35. M.A. Delichatsios, "The Flow of Fire Gases Under a Beamed Ceiling," *Combustion and Flame,* 43, 1 (1981).
36. C. Koslowski and V. Motevalli, "Behavior of a 2-Dimensional Ceiling Jet Flow: A Beamed Ceiling Configuration," *Fire Safety Science, Proceedings of the Fourth International Symposium* (T. Kashiwagi,

ed.), International Association of Fire Safety Science, Bethesda, MD, p. 469 (1994).
37. C.C. Koslowski and V. Motevalli, "Effects of Beams on Ceiling Jet Behavior and Heat Detector Operation," *Journal of Fire Protection Engineering,* 5, 3, p. 97 (1993).
38. B. Lattimer and U. Sorathia, "Thermal Characteristics of Fires in a Noncombustible Corner," *Fire Safety Journal*, 38, p. 709 (2003).
39. D. Coutts, "An Emissive Power Correlation for Solid Fuel Packages," *Journal of Fire Protection Engineering*, 21, p. 133, 2011.
40. D.D. Evans, "Thermal Actuation of Extinguishing Systems," *Combustion Science and Technology,* 40, p. 79 (1984).
41. D.D. Evans, "Calculating Sprinkler Actuation Time in Compartments," *Fire Safety Journal*, 9, 147 (1985).
42. L.Y. Cooper, "A Buoyant Source in the Lower of Two Homogeneous, Stably Stratified Layers," *20th International Symposium on Combustion,* Combustion Institute, Pittsburgh, PA (1984).
43. E.E. Zukoski and T. Kubota, "An Experimental Investigation of the Heat Transfer from a Buoyant Gas Plume to a Horizontal Ceiling—Part 2: Effects of Ceiling Layer," *NBS-GCR-77-98,* National Bureau of Standards, Washington, DC (1977).
44. W.D. Davis, "The Zone Fire Model Jet: A Model for the Prediction of Detector Activation and Gas Temperature in the Presence of a Smoke Layer," *NISTIR 6324,* National Institute of Standards and Technology, Gaithersburg, MD (1999).
45. L.Y. Cooper, "Estimating the Environment and the Response of Sprinkler Links in Compartment Fires with Draft Curtains and Fusible Link-Actuated Ceiling Vents—Theory," *Fire Safety Journal,* 16, pp. 137–163 (1990).
46. E.E. Zukoski, T. Kubota, and C.S. Lim, "Experimental Study of Environment and Heat Transfer in a Room Fire," *NBS-GCR-85-493,* National Bureau of Standards, Washington, DC (1985).
47. H.W. Emmons, "The Ceiling Jet in Fires," *Fire Safety Science, Proceedings of the Third International Symposium* (G. Cox and B. Langford, eds.), Elsevier Applied Science, New York, p. 249 (1991).
48. W.R. Chan, E.E. Zukowski, and T. Kubota, "Experimental and Numerical Studies on Two-Dimensional Gravity Currents in a Horizontal Channel," *NIST-GCR-93-630,* National Institute of Standards and Technology, Gaithersburg, MD (1993).
49. G. Heskestad, "Propagation of Fire Smoke in a Corridor," *Proceedings of the 1987 ASME/JSME Thermal Engineering Conference,* Vol. 1, American Society of Mechanical Engineers, New York (1987).
50. T. Hara and K. Shinsuke, "Numerical Simulation of Fire Plume-Induced Ceiling Jets Using the Standard $\kappa - \varepsilon$ Model," *Fire Technology,* 42, p. 131 (2006).

Dr. Ronald L. Alpert received his undergraduate and graduate education at the Massachusetts Institute of Technology, where he majored in mechanical engineering. For nearly 35 years, he was with FM Global in various technical and managerial positions, ending his career there as an assistant vice president and manager of the Flammability Technology Research Program. Dr. Alpert was editor in chief of the *Journal of Fire Protection Engineering for 10 years and a section editor of the NFPA Fire Protection Handbook, 20th edition. He has published numerous papers in refereed journals and technical reports.*